Published in Renewable Energy with doi: 10.1016/j.renene.2024.120300

Best-Case-Aware Planning of Photovoltaic-Battery Systems for Multi-Mode Charging Stations

Marcos Tostado-Véliz[1], Ahmad Rezaee Jordehi[2], Yuekuan Zhou[3,4,5,6], Seyed Amir Mansouri[7], Francisco Jurado[1,*]

1. Department of Electrical Engineering, University of Jaén, 23700, Linares, Spain (e-mail: mtostado@ujaen.es (M.T.-V.) and fjurado@ujaen.es (F.J.))
2. Department of Electrical Engineering, Rasht Branch, Islamic Azad University, Rasht, Iran (e-mail: ahmadrezaeejordehi@gmail.com).
3. Sustainable Energy and Environment Thrust, Function Hub, The Hong Kong University of Science and Technology (Guangzhou), Nansha, Guangzhou, 511400, Guangdong, China (e-mail: yuekuanzhou@ust.hk).
4. Department of Mechanical and Aerospace Engineering, The Hong Kong University of Science and Technology, Clear Water Bay, Hong Kong SAR, China
5. Division of Emerging Interdisciplinary Areas, The Hong Kong University of Science and Technology, Clear Water Bay, Hong Kong SAR, China
6. HKUST Shenzhen-Hong Kong Collaborative Innovation Research Institute, Futian, Shenzhen, 518048, China
7. Institute for Research in Technology (IIT), ICAI School of Engineering, Comillas Pontifical University, 28015 Madrid, Spain (e-mail: amir.mansouri24@gmail.com).

Abstract. The proliferation of charging stations entails multiple challenges for power systems. In this regard, the installation of photovoltaic-battery systems may help to mitigate the negative effects of charging points. However, such assets should be carefully planned, paying attention to economic aspects, principally. Most of existing works optimize the photovoltaic-battery system in charging infrastructures taking a representative-space of the involved variables (e.g. photovoltaic potential, charging demand or energy prices). However, this approach tends to ignore low-probable scenarios. Thus, the best-case scenario for charging demand (i.e. that for which the highest charging profit is accessible) may not be included in the analysis and therefore such demand could be not attended properly, thus losing this monetary opportunity. This paper focuses on this issue and questions if considering the best-case scenario into planning photovoltaic-battery systems for charging stations is worthwhile or not. To this end, a novel best-case-aware planning tool is developed, including the best-case scenario through a novel chance-constrained formulation. The overall problem is then decomposed into a master-slave structure by which the economy of the system is optimized together with the number of scenarios for which the best-case profile can be attended. A case study serves to validate the developed tool and shed light on the questions arisen in this work. In particular, it is checked that considering the best-case scenario into planning tools is questionable from a monetary point of view. Nevertheless, its inclusion unlocks some collateral advantages such as incrementing the users' satisfaction or reducing the grid-dependency.

Keywords. Battery energy storage; Chance-constrained programming; Electric vehicle; Photovoltaic energy; Renewable energy

Nomenclature

Indices (sets)	
$s(\mathcal{S})$	Scenario
$t(\mathcal{T})$	Time
$r(\mathcal{R})$	Representative day
Ω_r	Cluster of the r^{th} representative day
Superscripts	
PV	Photovoltaic
$BES, c/d$	Battery energy storage in charging/discharging mode
$Grid, I/E$	imported/exported from/to the grid
$EV, F/SF$	Fast/semi-fast charging of electric vehicles
$\underline{(\cdot)}/\overline{(\cdot)}$	Minimum/maximum value of a variable or parameter
$\widetilde{(\cdot)}$	Non-deterministic parameter represented by representative days
Parameters	
ϑ	Solar irradiance [kW/m²]
θ	Ambient temperature [ºC]
i	Interest rate [pu]
Y	Project lifetime [years]
κ	Capital and installation costs [$/kW or $/kWh]
$\Delta\tau$	Time step [h]
λ	Energy price [$/kWh]
δ	Reduction of the exporting price compared to the importing one [pu]
m	Operation and maintenance cost [$/kWh]
η	Efficiency [pu]
μ	Charging price [$/kWh]
Π	Budget [$]
$\mathrm{P}^{PV}/\mathrm{E}^{BES}$	Maximum installable capacity of photovoltaic panels/ batteries [kW/kWh]
e2P	Energy-to-power ratio [h]
DOD	Depth-of-discharge [pu]
Decision variables	
$\overline{p}^{PV}/\overline{\epsilon}^{BES}$	Capacity of photovoltaic panels/batteries [kW/kWh]
p	Power [kW]
ϵ	Energy [kWh]
α	Loss of opportunity factor [pu]

1 - Introduction

1.1- Context and motivation

Sales of electric vehicles (EVs) have steadily grown during the last decade. Actually, the total number of sales doubled in 2021 from the previous year, incrementing the EV stock to more than 16 million worldwide [1]. However, the increment in EV sales is not accompanied by a proper deployment of charging infrastructures, which are still limited in some countries [2]. In this context, the number of charging points should increment notably in the following years.

1.2 - The importance of renewable and storage integration in charging stations

Currently, fast and ultra-fast charging modes reach until 400 kW, being 20-50 kW the most common range in existing installations [3]. This scenario entails stressful conditions for existing power networks, which will see a dramatic load increment, eventually concentrated in some areas and with particular very high-peak power consumption periods [4].

In this context, installing renewable sources and storage systems near to charging points may mitigate their harmful impact on the network. Indeed, renewable generators could reduce the net demand by increasing self-consumption of charging infrastructures, whereas energy storage should contribute to reduce peak consumption and flatten the demand curve [5].

1.3 - Planning of charging stations with renewables and energy storage: state-of-art

It is evident that charging stations should be properly designed. Especially, optimal planning strategies may help to maximize expected profit of such infrastructures. There exist a number of references focused on the optimal sitting of charging points in highways or particular routes (see e.g. [6] and references therein). However, we focus here on the optimal planning of renewable generators and energy storage systems for charging stations.

To properly plan an installation over a long-time period (normally the expected project lifetime), the input data regarding demand and weather parameters can be characterized in different ways. In this regard, a number of works assume profiles artificially generated through well-suited probability distributions. In particular, a mixed-integer-linear programming (MILP) framework was proposed in [7], for optimal sizing of battery energy storage (BES) in fast charging stations. Mirhoseini and Ghaffarzadeh [8] developed a linear-programming (LP) model for optimal BES planning in semi-fast grid-connected charging stations from an economic point of view. Reference [9] focuses on ultra-fast charging points and their particular demanding conditions, for which a MILP optimization model was proposed for optimal battery sizing. In contrast, reference [10] proposed a scenario-based approach for optimal planning of fully-green isolated charging stations equipped with photovoltaic (PV) and wind units, together with BES. In other cases, instead of recurring to generic probability distributions, specific models can be constructed. In this regard, a specific fast charging demand model was developed in [5], which build up charging profiles from daily mileage and trip probability functions inferred by real data in U.S.

Generating profiles from stochastic distributions is an acceptable option when real data is unavailable. However, when real databases or measurements are accessible, other alternatives can be used instead. In this sense, Hafez and Bhattacharya [11] consider the use of yearly databases to optimally design semi-fast charging stations with renewables and battery, for which the software HOMER was employed [12]. Similarly, reference [13] proposes two different data-driven models for optimal design of fast charging stations with PV and BES. When the available measurements span for long time periods thus encompassing a large amount of data, the problem may become intractable in practise. In such cases, specific solvers can deal with large databases efficiently, but analytic (i.e. exact) optimization methods may present unaffordable computational burden. To overcome this problem, the whole dataset can be reduced to an assumable set of representative profiles using clustering techniques. This approach was used in [14] for optimal

planning of ultra-fast charging stations and [15] for charging infrastructures equipped with flywheel storage systems.

Planning of PV-BES systems is normally casted as an optimization framework, which seeks for minimizing/maximizing the total project cost/profit [16, 17]. Nevertheless, some references focus on other secondary aspects such as uncertainties modelling. In this regard, uncertain solar generation and charging demand may have an impact on the final size of components. To quantify and diminish the impact of such uncertainties, robust programming was employed in [14]. In this way, the result of the problem can be considered inhibited of the impact of uncertainties. On the other hand, a risk-averse approach was established in [13], by which the profit loss due to uncertainties can be bounded using a well-suited metric. Similar, reference [18] uses chance-constrained programming, by which the result is robust under the realization of a bounded set of uncertainties realization.

It is worth noting that the optimal planning of charging stations may result in complex formulations. In this regard, some references have proposed the use of metaheuristics to address the optimal sizing of PV-BES systems in charging infrastructures. Thus, genetic algorithms were used in [19], for optimally sizing PV units and batteries in fast charging stations, whereas a similar methodology was employed in [14] for ultra-fast infrastructures. Nevertheless, although metaheuristics can work well under some circumstances, analytic methods are normally preferred because of their versatility and capability to achieve the global optimum [20].

1.4 - Our questions

Mostly, references above optimize an installation over a set of scenarios for charging load and PV generation. Thus, the optimization problem considers such scenarios as possible realizations of the represented parameters, optimizing the installation for the most probable occurrence. This way, when a database is reduced to a set of representative days, the optimization tool assumes that the projected installation will work under these representative profiles during its entire lifetime, while the other possible realizations are ignored as they are considered to be represented by clustering data. However, this data characterization tends to ignore low-probable extreme cases as clustering techniques frequently neglect them naturally [21]. For the particular case of charging stations, the clustering process may throw away the so-called ‘best-case charging scenario’ (i.e. the charging profile for which the highest possible profit is expected). This aspect is especially relevant since, if the PV-BES system is not properly designed, the best-case scenario could be not fully satisfied and therefore the highest-profit opportunity is not accessible. Brought up this particular situation, we raise two questions:

- If the best-case scenario for charging demand is taken into account in the planning process, do the final results vary notably?
- Is the best-case scenario worth considering in optimal planning tools for charging stations?

1.5 - Specific contributions

In this paper, we aim at properly responding the questions above. To this end, the contributions of this work are twofold:

- Developing an optimal planning tool for PV-BES systems in multi-mode charging stations considering the best-case scenario for charging demand. Thereby, the developed tool seeks for minimizing the expected project cost, but being prevented to satisfy the considered best-case demand if it occurs. To this end, an original master-slave optimization framework is developed, in which the best-case scenario is embedded into the problem using chance-constrained programming.
- Obtaining different numerical results on a benchmark case study to analyse how the consideration of the best-case charging demand affects to the final optimization results,

as well as discussing if considering this scenario in the planification process is worthwhile.

1.6 – Differences with [4] and paper organization

Given the title of the present paper, the reader may reach the conclusion that the present work and [4] are rather similar and therefore the new proposal supposes a marginal contribution. However, there are notable differences between these two works. For simplicity, we point out them below:

- [4] focuses on day-ahead scheduling whereas the present work is devoted on planning purposes. In this sense, while ref. 4 raises a model to be executed within 24 hour time windows, the present work focuses on long time horizons (years). Moreover, the size of the PV-BES systems is considered a parameter rather than a decision variable in [4], as such, that model does not actually optimizes the size of components.
- In [4], uncertainties are modelled via a hybrid stochastic-interval approach, wherein charging demand is modelled via scenarios while PV potential and energy prices are determined by confidence bounds (robust optimization). In this sense, the present work differs from that model in [4] due to we do not consider interval notation in the developed model.
- In [4], the best-case scenario is not considered in the model and therefore it is expected that clustering techniques employed in this reference naturally ignores this case. The present work proposes an original optimization model to consider the best-case demand and design the system consequently.
- The developed master-slave solution framework is original and not used in [4].
- The case study in [4] focuses mainly on the impact of uncertainties, while the present work rather focuses in the effect of considering the best-case demand within the planning framework or not.

As seen, the model developed in this paper is rather different to that proposed in [4]. Albeit both papers focus on the optimization of multi-mode charging stations, the mathematical models, scope and time horizons are quite different.

In the rest of this paper, Section 2 describes some preliminaries. Section 3 presents the mathematical formulation of the optimal PV-BES planning problem for charging stations. Section 4 explains the proposed modifications introduced to consider the best-case scenario for charging demand. Section 5 presents a case study with results. Finally, the paper is concluded with Section 6.

2 - Preliminaries

2.1 - Station overview and problem statement

This paper deals with the optimal planning of PV-BES systems for multi-mode charging stations. In this regard, we assume an already operative station, which does not count with PV-BES facility. Thus, the problem described in this paper consists on optimally designing these assets for self-supplying of charging demand. To this end, we assume that raw data regarding weather parameters, energy pricing and charging demand is available for an acceptable time span (one year).

Fig. 1 depicts the considered charging infrastructure. As seen, the station is connected to the local power grid, which is owned by a utility and by which can exchange energy. In addition, semi-fast and fast chargers are available in the station, being the most widely charging modes worldwide [3]. For these charging modes, mature charger technologies are available such as CCS or CHAdeMO, which allow charging in AC or DC. Once the PV-BES system is installed, the station could be partially self-supplied, which further redound in monetary savings and reducing energy imports.

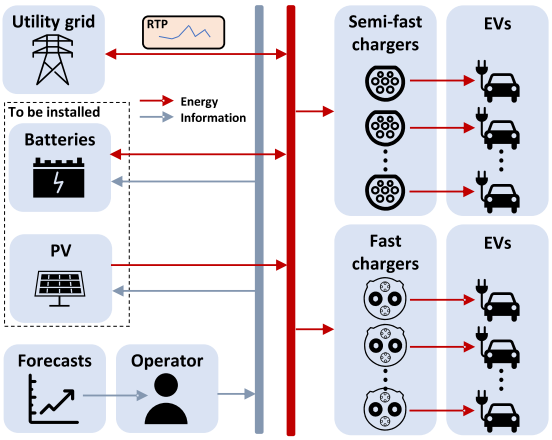

Fig. 1 - Schematic representation of the studied multi-mode charging station

2.2 - Assumptions

As commented, we assume that a considerable amount of data is available and can be used in the optimal planning tool. Thereby, such data can be used as input for the developed planning tool, thus resulting in a data-driven approach. Moreover, this work only accounts for the PV-BES installation, being out of scope the design or economic aspects related with other devices (e.g. chargers). In this regard, we assume that the PV-BES is installed in the first year of the project, which spans for a long-time period (~25 years [22]).

On the other hand, we assume that the considered installation adopts a price-taker strategy in local energy markets. Thus, both imports and exports from the local grid are subjected to market real-time-price (RTP). Finally, the whole installation is centrally managed by a charging operator or similar, who decides on optimal scheduling of the different devices within the installation. This way, the operator or scheduler seeks for the most economical operation of the whole system, taking into account the incomes from EV charging.

3 - Optimal PV-BES planning model for multi-mode charging stations

3.1 - Data characterization

In planning problems, a large amount of data has to be managed. These data typically span for long time periods, thus entailing challenging computational frameworks. The input data typically encompass energy pricing, weather and demand profiles. Within a specific database, different profiles can share similar features, which allows to reduce the original scenario-space into a minimal accurate representation of the whole dataset. This practise is known as 'representative days' and is used in this paper to reduce the yearly information regarding weather, prices and demand to a tractable set of representative profiles.

Thus, we start from a dataset of weather measurements. In our problem, solar irradiance and air temperature are needed to estimate the instantaneous PV potential, which can be calculated using the following panel model [23].

$$\tilde{\varphi}_{s|t}^{PV} = 0.2 \cdot \tilde{\vartheta}_{s|t} + 0.024 \cdot \tilde{\vartheta}_{s|t} \cdot \tilde{\theta}_{s|t}; \forall s \in \mathcal{S} \wedge t \in \mathcal{T} \quad (1)$$

Equation (1) yields the PV potential at time t and scenario s per unit, which means that (1) can be multiplied by the peak power of PV panels to calculate the potential in kW.

Then, the PV potential together with the available data for charging demand and energy prices are collectively reduced using a well-known clustering technique. There are different approaches available in the literature [24]. In this paper, we use the k-medoids technique, which typically offers good features [25] and has been used in other similar works [26].

One of the main issues of the k-medoids is the necessity of specifying the number of clusters a priori. This may be difficult since this parameter should be set carefully in order to keep the

model tractable without losing accuracy. To this end, we use the methodology described in [27], which combines the elbow method with triangle threshold.

3.2 - Detailed formulation

Below, we present the detailed formulation of the optimal PV-BES planning model for multi-mode charging stations, which will be further developed to account for the best-case scenario for charging demand.

$$\min_{\boldsymbol{x},\boldsymbol{y}_r;\forall r\in\mathcal{R}} \left\{ \underbrace{\frac{i\cdot(1+i)^Y}{(1+i)^Y-1}\cdot\left(\kappa^{PV}\cdot\overline{p}^{PV}+\kappa^{BES}\cdot\overline{\epsilon}^{BES}\right)}_{Capital\ costs}+ \sum_{r\in\mathcal{R}}|\Omega_r|\cdot\Delta\tau\cdot\sum_{t\in\mathcal{T}}\left[\underbrace{\tilde{\lambda}_{r|t}\cdot\left(p_{r|t}^{Grid,I}-\delta\cdot p_{r|t}^{Grid,E}\right)}_{Energy\ exchanged\ with\ the\ grid}+ \underbrace{m^{BES}\cdot\left(p_{r|t}^{BES,c}\cdot\eta^{BES,c}+\frac{p_{r|t}^{BES,d}}{\eta^{BES,d}}\right)}_{Degradation\ of\ batteries}- \underbrace{\left(\mu^{EV,F}\cdot p_{r|t}^{EV,F}+\mu^{EV,SF}\cdot p_{r|t}^{EV,SF}\right)}_{Incomes\ from\ charging\ vehicles} \right] \right\} \tag{2}$$

Subject to:

$$\kappa^{PV}\cdot\overline{p}^{PV}+\kappa^{BES}\cdot\overline{\epsilon}^{BES}\leq\Pi \tag{3a}$$

$$\overline{p}^{PV}\leq \mathrm{P}^{PV},\ \overline{\epsilon}^{BES}\leq \mathrm{E}^{BES} \tag{3b}$$

$$p_{r|t}^{Grid,I}+p_{r|t}^{PV}+p_{r|t}^{BES,d}=p_{r|t}^{Grid,E}+p_{r|t}^{BES,d}+p_{r|t}^{EV,F}+p_{r|t}^{EV,SF};\forall r\in\mathcal{R}\wedge t\in\mathcal{T} \tag{4a}$$

$$\epsilon_{r|t}^{BES}=\epsilon_{r|t-1}^{BES}+\Delta\tau\cdot\left(p_{r|t}^{BES,c}\cdot\eta^{BES,c}-\frac{p_{r|t}^{BES,d}}{\eta^{BES,d}}\right);\forall r\in\mathcal{R}\wedge t\in\mathcal{T}\backslash t=1 \tag{4b}$$

$$\epsilon_{r|1}^{BES}=\epsilon_{r|\mathcal{T}|}^{BES}=\overline{\epsilon}^{BES};\forall r\in\mathcal{R} \tag{4c}$$

$$p_{r|t}^{Grid,j}\leq\overline{p}^{Grid};\forall r\in\mathcal{R}\wedge t\in\mathcal{T}\wedge j\in\{I,E\} \tag{5a}$$

$$p_{r|t}^{BES,j}\leq\frac{\overline{\epsilon}^{BES}}{\mathrm{e2P}};\forall r\in\mathcal{R}\wedge t\in\mathcal{T}\wedge j\in\{c,d\} \tag{5b}$$

$$p_{r|t}^{PV}\leq\tilde{\varphi}_{r|t}^{PV}\cdot\overline{p}^{PV};\forall r\in\mathcal{R}\wedge t\in\mathcal{T} \tag{5c}$$

$$p_{r|t}^{EV,j}\leq\tilde{p}_{r|t}^{EV,j};\forall r\in\mathcal{R}\wedge t\in\mathcal{T}\wedge j\in\{F,SF\} \tag{5d}$$

$$(1-\mathrm{DOD})\cdot\overline{\epsilon}^{BES}\leq\epsilon_{r|t}^{BES}\leq\overline{\epsilon}^{BES};\forall r\in\mathcal{R}\wedge t\in\mathcal{T} \tag{5e}$$

The objective function (2) minimizes the total project cost, which is equivalent to maximize the total profit. In particular, (2) encompasses the capital costs, which include the installation costs due to the installation of PV panels and batteries. It is worth noting that the capital costs are annualized over the project lifetime Y assuming an interest rate i [28].

In addition, (2) includes the operational costs in which incurs the installation daily. The first of these terms account for the energy exchanged with the grid. Thus, this term includes expenditures from imports and incomes from exports. Note that the exported power is multiplied by a term $\delta<1$, which forces the selling price to be lower than the importing one, as customary in real markets [29]. The second term represents the degradation costs of batteries, which has been considered a linear function of the energy exchanged through the BES system [30]. Lastly, incomes from providing charging services are also accounted, considering different charging prices for semi-fast and fast charging modes, respectively, as usual in real installations [31]. Note that operational costs are multiplied by the size of each cluster. This way, such costs are represented over a year basis.

The problem is completed by the project constraints (3). In particular, (3a) is the budget constraint, which bounds the capital costs to a predetermined available budget, whereas (3b) limits

the installed capacity of PV panels and batteries. This last constraint represents possible limitations in space that can restrict the deployment of panels and batteries in real installations.

The rest of the constraints are the equality (4) and inequality (5) operational constraints, respectively. In particular, (4a) is the power balance while (4b) represents the instantaneous state-of-charge (SOC) of the BES system. Since (4b) is not defined at the beginning of the time horizon, (4c) fixes the initial and final SOC to keep the model coherent. Regarding (5), this set of constraints represent equipment limits. Thus, (5a) limits the power exchanged with the grid while (5b) establishes the power rate of batteries as a function of the total capacity and the energy-to-power ratio [29]. Similar, (5c) limits the PV generation to the calculated PV potential in (1) multiplied by the peak power of PV panels. Finally, (5d) limits the charging demand satisfied, in the way as the model above allows to reject or partially satisfy charging events for convenience, while (5e) limits the SOC of the BES system to its nominal capacity and depth-of-discharge (DOD) settings.

Finally, it is worth commenting that binary commitment variables are not included in (6) since the efficiency of batteries is lower than 1 and selling prices are always lower than the purchasing ones [32]. This way, (6) results in a LP framework that can be easily solved using off-the-shelf solvers.

3.3 - Compact notation

For convenience, we present below the matrix notation of the problem (2)-(5).

$$\min_{\boldsymbol{x},\boldsymbol{y}_r;\forall r\in\mathcal{R}} \frac{i\cdot(1+i)^Y}{(1+i)^Y-1}\cdot(\boldsymbol{\kappa}^T\cdot\boldsymbol{x})+\sum_{r\in\mathcal{R}}|\Omega_r|\cdot\boldsymbol{d}_r^T\cdot\boldsymbol{y}_r \tag{6a}$$

Subject to:

$$\boldsymbol{\kappa}^T\cdot\boldsymbol{x}\leq\Pi \tag{6b}$$

$$\left[\overline{p}^{PV},\overline{\epsilon}^{BES}\right]\leq[\mathrm{P}^{PV},\mathrm{E}^{BES}] \tag{6c}$$

$$\boldsymbol{h}(\boldsymbol{x},\boldsymbol{y}_r)=\boldsymbol{0};\forall r\in\mathcal{R} \tag{6d}$$

$$\boldsymbol{g}(\boldsymbol{x},\boldsymbol{y}_r)\leq\boldsymbol{0};\forall r\in\mathcal{R} \tag{6e}$$

Indeed, (6a) is the objective function, (6b) and (6c) represent the project constraints (3), (6d) encompasses the equality operational constraints (4), while (6e) are the operational inequality constraints (5).

4 - The proposed planning model

4.1 - Best-case selection

The problem (6) only accounts for the representative profiles encrypted into the set $\mathcal{R}$. This data characterization, although useful, typically filter some extreme profiles due to their eventual low probability of occurrence. For instance, we verified in previous experiments that the so-called best-case scenario for charging demand is typically filtered when using the k-medoids technique.

In subsequent sections, we present an original formulation to modify the problem (6) in order to account for the best-case charging demand. In particular, this scenario is defined as that for which the highest profit for EV charging is accessible. Hence, the best-case profile is defined in (7) and its instantaneous charging demand is given by (8).

$$\mathcal{S}^{EV,best}\leftarrow\max_{\forall s\in\mathcal{S}}\left\{\Delta\tau\cdot\sum_{t\in\mathcal{T}}\left[\mu^{EV,F}\cdot p_{s|t}^{EV,F}+\mu^{EV,SF}\cdot p_{s|t}^{EV,SF}\right]\right\} \tag{7}$$

$$p_t^{EV,best}=p_{\mathcal{S}^{EV,best}|t}^{EV,F}+p_{\mathcal{S}^{EV,best}|t}^{EV,SF};\forall t\in\mathcal{T} \tag{8}$$

To illustrate how the k-medoids performs and the importance of including the best-case in our planning problem, we generated 365 charging scenarios using the technique described in [4] (taking the station characteristics given in Section 5). Then, the k-medoids was employed to reduce the original 365 scenarios to 11 representative profiles, which are plotted in Fig. 2 together

with the best-case calculated using (8). As seen, the representative profiles are not aware about some particular features of the best-case scenario. Indeed, peak charging demand at evening is not captured by any representative scenario. In addition, the best-case scenario presents a permanent high demand (~150 kW), which is not reflected by any other profile in which power demand frequently falls to zero or very low values.

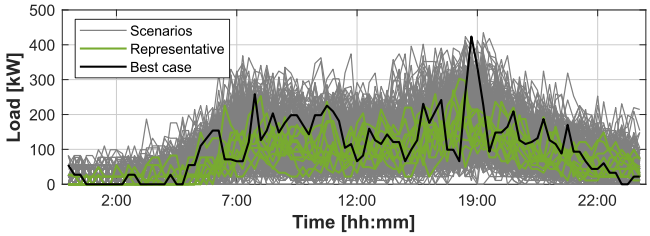

Fig. 2 - Illustrative example about the importance of considering the best-case scenario. As seen, the representative profiles do not capture some important features of the best-case profile

4.2 - Formulating the best-case as a chance-constrained programming

As seen in the previous section, data reduction techniques are not adequate to capture the best-case demand scenario. In this section, we aim at including the best-case scenario into the optimal PV-BES planning model (6). The simplest way to do that is including the best-case as an independent scenario with associated probability. Nevertheless, this approach will undoubtedly lead to oversizing the PV-BES system. Indeed, adopting this approach would force the result of (6) to satisfy the best-case demand even under scenarios with low PV potential. Note that such scenarios might be improbable in practise and therefore and therefore the solution should not be uniquely ruled by them [33].

In this regard, we aim at developing a tool suitable to consider the best-case scenario without oversizing the PV-BES system unnecessarily. To this end, we propose hereafter an original chance-constrained formulation of the best-case scenario. Chance-constrained programming is a very popular formulation-oriented approach in scenario-based optimization tools, which ensures that some constraints or objectives are met for a predefined number of scenarios [34]. This way, instead of forcing to fully satisfy the best-case demand, the proposed formulation ensures that this profile is, at least, covered up to a given portion.

Intuitively, the chance-constrained idea matches with the requirements of the developed best-case aware approach. Specifically, we aim at ensuring that the best-case scenario can be satisfied using own assets for a given number of scenarios. Formally, this idea can be stated as

$$\Pr\left\{p_t^{EV,best} - \tilde{\varphi}_{r|t}^{PV} \cdot \overline{p}^{PV} - \frac{\overline{\epsilon}^{BES}}{\mathrm{e2P}} \geq 0\right\} \leq \alpha_r; \forall r \in \mathcal{R} \tag{9}$$

Equation (9) indicates that the portion of the best-case demand that can be covered by own assets is higher than a predefined bound given by α_r. Thus, the parameter α_r, which will be called loss opportunity factor (LOF), lower bounds the probability of meeting the best-case scenario for a given a PV-BES size. For instance, a value of $\alpha = 0.2$ points out that a 20 % of the total best-case demand cannot be satisfied through the PV-BES system.

Therefore, our objective is calculating the most-economical PV-BES system that minimizes the LOF. However, (9) is non-convex and has not a closed form, being few applicable in optimization problems. Instead, we convert (9) into a linear expression using the sampling average approach, as follows [34]

$$\frac{\sum_{t\in\mathcal{T}}\left[p_t^{EV,best} - \tilde{\varphi}_{r|t}^{PV} \cdot \overline{p}^{PV} - \frac{\overline{\epsilon}^{BES}}{\mathrm{e2P}}\right]}{\sum_{t\in\mathcal{T}} p_t^{EV,best}} \leq \alpha_r; \forall r \in \mathcal{R} \tag{10}$$

Note that we consider the LOF scenario-dependent due to the presence of the PV potential at the left-hand side of (10).

4.3 - Proposed master-slave solution strategy

Our proposal faces two different objectives. On the one hand, we aim at minimizing the LOF in order to meet the best-case for a large number of scenarios. On the other hand, the PV-BES should be sized so that the total project cost/profit is minimized/maximized. To address these two targets on a whole, we propose a master-slave solution strategy, whose main idea is sketched in Fig. 3, while further details are given below.

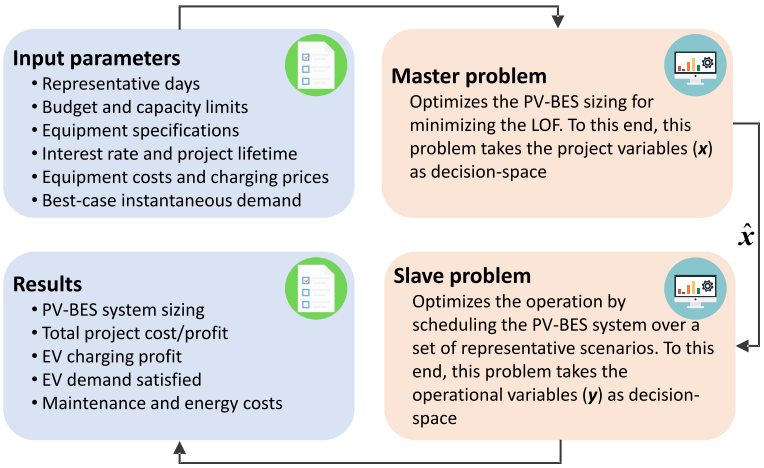

Fig. 3 - Sketch of the developed master-slave solution procedure

The master problem optimizes the project-related variables, i.e. the PV-BES sizing, with the unique objective of reducing the LOF. Thus, the resulted PV-BES planning is optimized only from a risk perspective, while economy is only accounted in the budget constraint, which ensures that the capital cost does not exceed the available budget. Under these premises, the master problem of our developed solution strategy is raised, as follows:

$$\hat{\boldsymbol{x}} \leftarrow \underset{\boldsymbol{x},\alpha_r;\forall r\in\mathcal{R}}{\operatorname{argmax}}\ 1-\sum_{r\in\mathcal{R}}\frac{|\Omega_r|}{365}\cdot\alpha_r \tag{11a}$$

Subject to:

$$\boldsymbol{\kappa}^T\cdot\boldsymbol{x}\le\Pi \tag{11b}$$

$$\left[\overline{p}^{PV},\overline{\epsilon}^{BES}\right]\le\left[\mathrm{P}^{PV},\mathrm{E}^{BES}\right] \tag{11c}$$

$$\frac{\sum_{t\in\mathcal{T}}\left[p_t^{EV,best}-\tilde{\varphi}_{r|t}^{PV}\cdot\overline{p}^{PV}-\frac{\overline{\epsilon}^{BES}}{\mathrm{e2P}}\right]}{\sum_{t\in\mathcal{T}}p_t^{EV,best}}\le\alpha_r;\forall r\in\mathcal{R} \tag{11d}$$

$$0\le\alpha_r\le 1;\forall r\in\mathcal{R} \tag{11e}$$

It is noteworthy that the objective function in (11) does not consider the LOF directly. Instead, (11a) maximizes the opposite to the LOF so that a higher value of the objective function implies a lower LOF. Moreover, the probability of occurrence of each r^{th} scenario (i.e. the number of days that the r^{th} scenario is expected to occur over a year) is explicitly included in the objective function. This way, the importance of each scenario is weighted by its probability of occurrence. By this approach, we reduce the impact of low-probable scenarios on final results.

As seen, (11) decides on project variables ($\boldsymbol{x}$), resulting in the PV-BES planning that minimizes the LOF ($\hat{\boldsymbol{x}}$). Regarding the constraints above, (11b) and (11c) are the same as (6b) and (6c), respectively. On the other hand, (11d) and (11e) integrate the chance-constrained formulation described in the previous section.

Note that the LOF is taken as a decision variable in (11). It is worth noting that in other chance-constrained problems, the LOF is a parameter tuned up by the operator or decision maker. However, this approach is not suitable in our particular case since a high value of the LOF may lead to infeasibility due to the constraints (11b) and (11c). Indeed, the available budget and

capacity limits actually lower bound the value of the LOF. On the other hand, considering the LOF a decision variable rather than a parameter makes this value to be problem-ruled rather than tuned by the operator. In this sense, the result of the problem is not enforced to meet a specific value of the LOF and therefore the system is optimized without oversizing components unnecessarily.

Finally, it is interesting to note that (11) does not force to fully cover the best-case demand. Instead, the problem (11) seeks for the PV-BES size that ensures that a portion α of the best-case scenario is covered by own resources. This approach avoids oversize the installation.

For a given PV-BES sizing, the slave problem focuses on the operational problem, deciding on the operational variables ($\boldsymbol{y}$) and accounting for operational constraints (6d) and (6e). Thereby, this problem focuses on operational decisions (i.e. energy, maintenance and charging profit). Thus, the slave problem reads as

$$\min_{\boldsymbol{y}_r;\forall r\in\mathcal{R}} \sum_{r\in\mathcal{R}} |\Omega_r| \cdot \boldsymbol{d}_r^T \cdot \boldsymbol{y}_r \tag{12a}$$

Subject to:

$$\boldsymbol{h}(\hat{\boldsymbol{x}}, \boldsymbol{y}_r) = \boldsymbol{0}; \forall r \in \mathcal{R} \tag{12b}$$
$$\boldsymbol{g}(\hat{\boldsymbol{x}}, \boldsymbol{y}_r) \leq \boldsymbol{0}; \forall r \in \mathcal{R} \tag{12c}$$

As seen, the objective function (12a) minimizes the operational-related costs while (12b) and (12c) collect the operational constraints, i.e. power and energy balances together with equipment limits, respectively. The main difference between (12) and (6) is that the former is optimized for a given PV-BES sizing ($\hat{\boldsymbol{x}}$), while (6) includes the project variables within its decision-space.

Note that, by the proposing master-slave decomposition, the project and operational variables are optimized in different problems with different objectives. This way, while the single-level problem (6) optimizes all the variables on a whole, our approach splits the planning framework, differentiating planning and operational objectives. Note that this approach aligns with other planning problems in power systems [35].

4.4 - Summary of differences between (6) and (11)-(12)

In (6), the size of the PV-BES system is optimized through a conventional single-level optimization framework. To this end, daily parameters such as solar irradiance or charging demand are characterized using a representation based on representative days. This approach reduces the original scenario space (e.g. measures taken over a year) to a minimum set of representative profiles that can be considered an accurate representation of the original dataset. In other words, the results obtained after running (6) should be similar whether one considers the original scenario space (denoted by $\mathcal{S}$) or the representative space (denoted by $\mathcal{R}$). However, the size of $\mathcal{R}$ is typically much lower than the size of $\mathcal{S}$, with the consequent computational advantages.

Unlike to (6), the model (11)-(12) considers the best-case scenario (in addition to $\mathcal{R}$). To this end, the best-case demand is explicitly included by $p_t^{EV,best}$ in the master problem (11). This problem determines the size of the PV-BES system so that a portion of the best-case demand is covered up to a value of $1 - \sum_{r\in\mathcal{R}} \frac{|\Omega_r|}{365} \cdot \alpha_r$ (objective function of (11)). This way, the problem (11) determines the PV-BES size that effectively can cover the demand in the best-case scenario, thus ensuring that monetary opportunities in this case are not lost.

Therefore, the main difference between these two models lie in the fact that (6) ignores the best-case demand and therefore the resulting PV-BES system could be unable to satisfy these charging events in case of happening. This issue can be seen clearly in Fig. 10, where the total charging incomes in the best-case scenario are compared for the two models. As seen, using the model (11)-(12) leads to obtain a higher profit in the best-case scenario, which indicates that the best-case demand is further covered when the system is optimized using that optimization model.

5 - Case study

This section presents a case study with results in order to address the objectives of this work and response the questions raised in Section 1.4. To this end, the optimization models described in this paper were coded under Matlab R2021s and solved using Gurobi [36]. All the optimizations were run on an Intel® Core™ i7-10700 K with 32.00 GB RAM. The operational problem is solved for a 24 hour time horizon taking 15 minutes time resolution. Note that this time resolution is suitable to represent the charging demand of fast chargers [4].

5.1 - Input data

To build the representative-space, we use several databases that are publicly available. In particular, we took the outdoor temperature and solar irradiance in the year 2020 at Madrid (Spain) from [37]. As previously explained, these data can be converted to PV potential using (1). For RTP prices, we considered the hourly energy pricing at PJM FE Ohio on 2020 [38]. Finally, real charging demand databases are not easily accessible nowadays, especially for large-scale stations. In this regard, we generated 365 scenarios using the methodology described in [4], considering 20 fast and semi-fast chargers (40 charging points in total), and 50 fast/20 semi-fast events per day, while the other parameters were taken as in [4].

Taking the data described above, the original 365 scenarios were reduced to 11 representative profiles using the methodology described in [27], which are plotted in Fig. 4. Furthermore, Fig. 5 plots the instantaneous demand corresponding to the calculated best-case scenario. The rest of parameters are given in Table 1. Note that capital costs were taken from [12], while battery data were adapted from [39] and the interest rate is the same as in [28]. Lastly, the charging prices correspond to common values in Spain in the year 2022 [40].

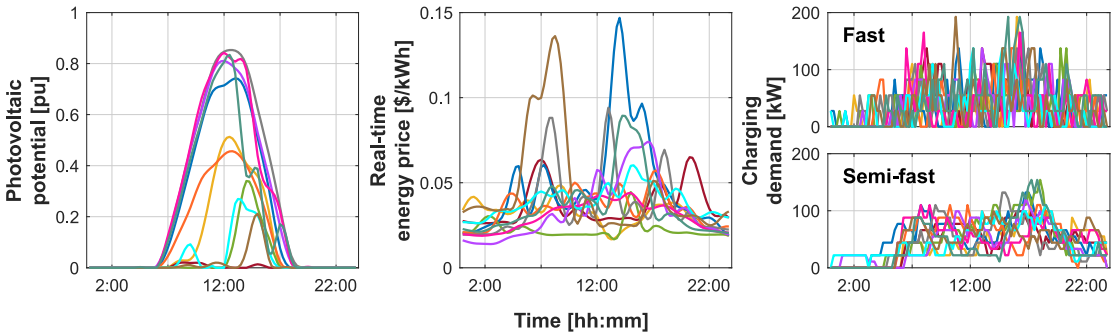

Fig. 4 - The representative profiles used in simulations

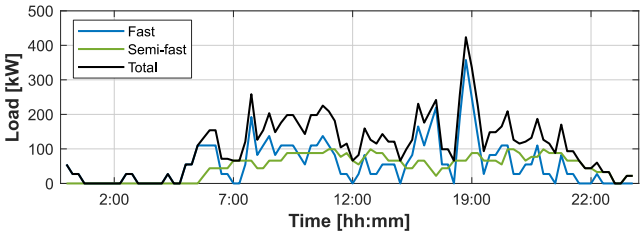

Fig. 5 - The best-case scenario for charging demand

Table 1 - Data used in simulations

Parameter	Value	Parameter	Value
κ^{PV}	1210 $/kW	P^{PV}/E^{BES}	150 kW/100 kWh
κ^{BES}	1242 $/kWh	e2P	2 hours
δ	0.9	DOD	0.7
m^{BES}	2.53 $/MWh	i	0.04
$\mu^{EV,F/SF}$	0.45/0.25 $/kWh	Y	25 years
$\eta^{BES,c/d}$	0.95	$\overline{p}^{Grid}$	150 kW

5.2 - PV-BES sizing analysis

We first analyse the main result of the developed solution approach, i.e. the PV-BES sizing. In this sense, Fig. 6 shows the value of the objective function (11a). As seen, the value of the objective function grows with the budget until reach maximum around 0.65. It indicates that, for the given parameters, the best-case demand can be satisfied through own assets by 65 %. After reaching this maximum at $\Pi = 350$ k$, the objective function does not further increase. It indicates that, for budgets below 350 k$, the PV-BES sizing is limited by the budget constraint and therefore more capacity can be installed by simply increasing the available budget. In contrast, the sizing constraint (11c) remains active and no more capacity can be installed for $\Pi > 350$ k$.

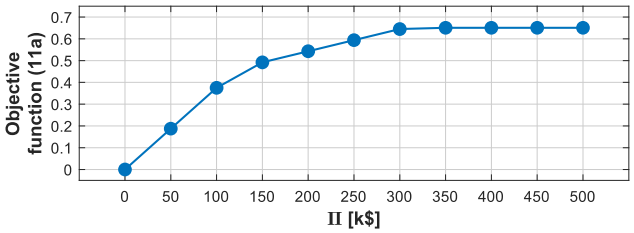

Fig. 6 - The value of the objective function (11a) for various budgets

To further analyse the results in Fig. 6, the PV and BES sizes for different budgets are shown in Fig. 7. In this case, we compare the results obtained with the single-level model (6), which can be considered as a benchmark and does account for the best-case scenario, with the developed tool (11)-(12). As observed, in the single-level model, both batteries and PV panels increase their capacity homogeneously until a maximum achieved at $\Pi = 100$ k$. It indicates that both assets contribute to reduce the total project cost, which is the unique objective in (6). It is also worth noting that, in this case, constraints (6b) and (6c) are inactive for $\Pi > 100$ k$. In contrast, BES capacity is firstly increased in the model (11)-(12) until (11c) is activated for batteries. Then, the PV size becomes increasing until reaching its maximum. This particular behaviour denotes a clear best-case-aware attitude. Indeed, the battery capacity contributes more notably to reduce the LOF in (11), since this asset is available any time instant unlike to PV limited to the availability of solar irradiance. These results show that, in the case of using the model (6), the PV-BES sizing is ruled by economic factors, while reducing the LOF is the most prominent objective in the model (11)-(12). In Fig. 7, it is also appreciated that no more capacity can be installed beyond $\Pi > 350$ k$ since the sizing constraint (11c) remains active beyond this point for both PV and BES units, which further validates the results reported in Fig. 6.

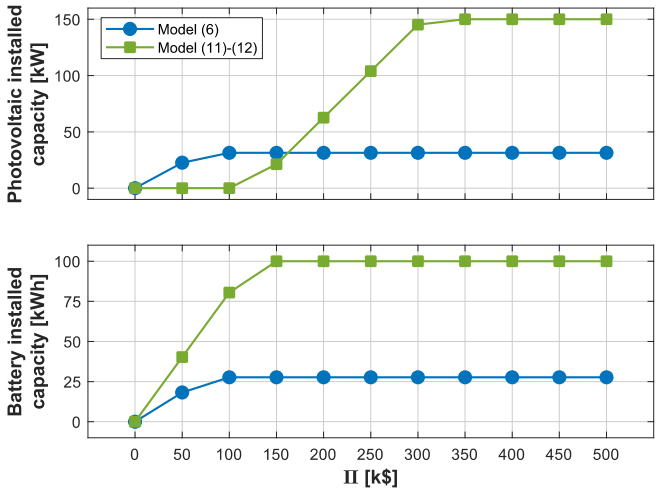

Fig. 7 - The PV-BES installed capacity for various budgets using the models (6) and (11)-(12)

5.3 - Cost analysis

Fig. 8 compares the annualized project cost for various budgets. As seen, the project cost is reduced with the model (6) until $\Pi = 100$ k$, keeping constant for any budget beyond that point. This result was expected since at $\Pi = 100$ k$ the PV-BES sizing is not further incremented. In contrast, the project cost is reduced when using our proposal until $\Pi = 50$ k$, increasing beyond that point. This is due to the differences in PV-BES sizing when comparing both models are marginal in terms of capital cost. Indeed, for $\Pi = 50$ k$, the PV-BES system resulted similar with both models in terms of total capacity. However, beyond this point, the BES is notably increased when using the model (11)-(12), while the PV array sizing is also notably incremented beyond $\Pi = 150$ k$.

Of course, considering the best-case scenario implies installing higher PV and storage capacity, as seen in Fig. 7. It is due to a higher onsite generation and storage capacity is needed to satisfy the best-case demand (i.e. $p_t^{EV,best}$). This has a direct impact on the total project cost, as seen in Fig. 8, since installing high-capacity components requires a higher capital investment. This is the reason why the model (6) gives rise a lower project cost in Fig. 7 when comparing with the model (11)-(12).

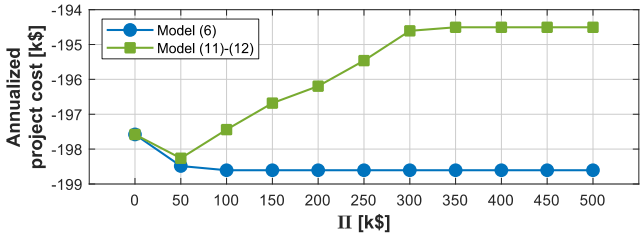

Fig. 8 - Total annualized project cost for various budgets

Thus, it is evident that (6) is only focused on reducing the costs. In contrast, the developed model is rather focused on satisfying the best-case scenario. Note that this is a critical point that should be carefully treated. Actually, investors should carefully evaluate whether considering the best-case scenario into the planning framework is worthwhile or not. In fact, it seems that including the best-case scenario in the model (11)-(12) does not offer any advantage and, in addition, the total project cost grows. However, the results obtained with our model allows to increment the total EV demand satisfied, as seen in Fig. 9, where the total annualized charging income is compared for the two models. Indeed, due to the higher PV-BES capacity, the installation is ready to further cover the charging demand not only in the best-case scenario, but also in the rest of scenarios in $\mathcal{R}$. This is the reason why the charging incomes are clearly higher when considering the best-case scenario. This is a key point when overall satisfaction of EV users is considered.

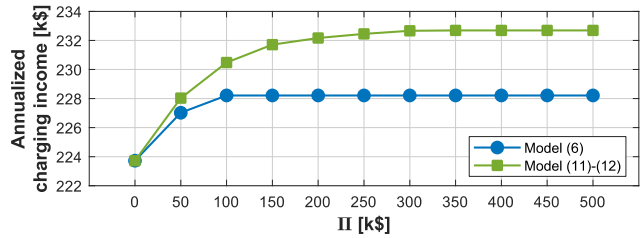

Fig. 9 - Total annualized charging income for various budgets

5.4 - Performance for the best-case scenario

One of the main features of the developed optimization framework is its capacity of considering the best-case and optimize the system in consequence. This aspect is analysed in Fig. 10, where the EV profit obtained for the best-case scenario is compared. As seen, the total incomes could be increased by ~50 $/day when considering the developed model.

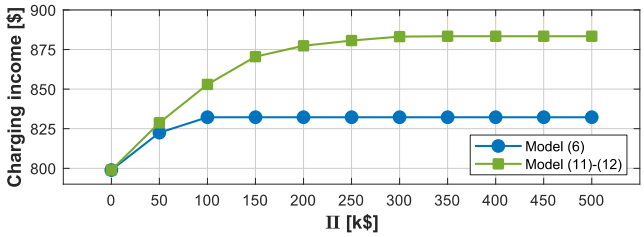

Fig. 10 - Total charging income for the best-case scenario

Therefore, we conclude that the total project cost is reduced when using the model (6), but charging incomes (especially when the best-case scenario appears) are higher when adopting the results obtained with the developed model. In this regard, a question arises: how many times should the best-case occurs to be worth of considering it? This key parameter is analysed in Fig. 11 for various budgets. As seen, the number of best-case occurrences per year should be higher than 50 in most of cases. In such a case, the best-case scenario could not be considered improbable and therefore the k-medoids method should naturally include it in the representative set of scenarios. Therefore, from a simple monetary point of view, the inclusion of the best-case scenario in the model is questionable.

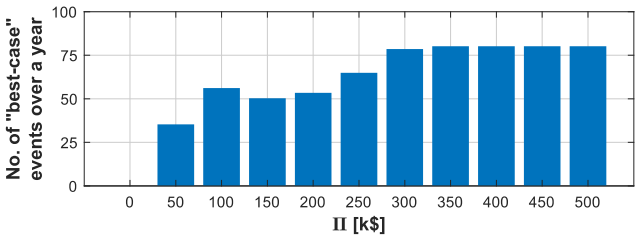

Fig. 11 - Number of best-case occurrences per year needed to compensate the extra project costs incurred when oversizing the PV-BES system after using the model (11)-(12)

5.5 - The effect of PV-BES on power imported

We compare the instantaneous power imported throughout a representative day with the models (6) and (11)-(12) in Fig. 12. As observed in this figure, the results obtained with the developed model allows to notably reduce the power imported, especially at midday, when PV potential is high. In this sense, the results obtained with the model (6) are more conservative and the reduced PV-BES size limits the 'peak-shaving' capacity of the installation. Actually, the peak power during midday is reduced to ~25 kW when using the model (11)-(12), while more than doubled with the results obtained with the model (6).

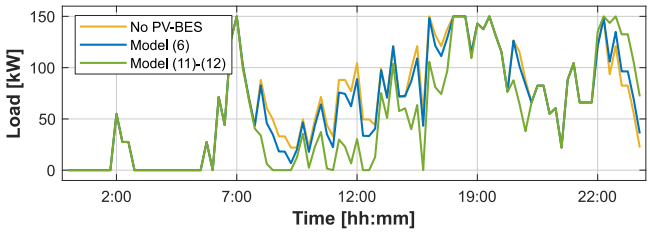

Fig. 12 - Power imported from the grid with various PV-BES layouts. In the case of models (6) and (11)-(12), results correspond with $\Pi = 400$ k$

Note that reducing the grid-dependency is especially relevant in a price-increasing context like that observed at the end of 2022. In this scenario, reducing the power imported from the grid is a key objective in order to diminish the impact of volatile energy prices. Nevertheless, a further study of this context is out of scope of this paper and we just shed light about some positive aspects of considering the best-case scenario in planning models.

5.6 - Research limitations and future studies

As commented previously, it remains to check whether the volatility of energy pricing in the long period impact notably in the developed PV-BES planning. Actually, it was shown that oversizing the PV-BES system contributes to reduce the grid-dependency of the installation. To this end, future works will be focused on modelling long-term variational energy prices and analyse different prospective scenarios.

6 - Conclusion

In this paper, a novel best-case-aware PV-BES planning model for multi-mode charging stations has been presented. The new proposal incorporates the best-case scenario for charging demand into the planning framework using an original chance-constrained approach. Then, the overall framework is decomposed into a master-slave structure, which allows to jointly optimize the total project cost and the number of scenarios for which the best-case scenario is satisfied. The results obtained in a case study shed light to the main questions raised in this work. Key conclusions are summarised below:

1. Considering the best-case scenario entails oversizing the PV-BES system, which increments the project cost by up to 3 %. In this regard, considering the best-case for charging demand into the planning tool is questionable from a monetary point of view.
2. Including the best-case scenario into the planning project is only profitable if more than 30 best-case events occur in a year. In such a case, the best-case scenario could not be considered improbable and clustering techniques should include it in the representative-space naturally.
3. Nevertheless, the results obtained demonstrated that considering the best-case scenario brings other secondary advantages such as a higher users' satisfaction and reduced grid-dependency. Moreover, up to 50 $ extra incomes are accessible for each best-case occurrence.

Future works should be focused on further investigating the potential of charging stations from a grid point of view, exploring its capability to provide ancillary services.

References

[1] IEA. Global EV Outlook 2022. Online, available at: https://www.iea.org/reports/global-ev-outlook-2022, (accessed on May 12, 2023).

[2] IEA. Trends in Charging Infrastructure. Online, available at: https://www.iea.org/reports/global-ev-outlook-2022/trends-in-charging-infrastructure, (accessed on May 12, 2023).

[3] U.S. Department of Energy. Electric Vehicle Charging Station Locations. Online, available at: https://afdc.energy.gov/fuels/electricity_locations.html#/find/nearest?fuel=ELEC, (accessed on May 12, 2023).

[4] M. Tostado-Véliz, S. Kamel, H.M. Hasanien, P. Arévalo, R.A. Turky, F. Jurado. A stochastic-interval model for optimal scheduling of PV-assisted multi-mode charging stations. *Energy* 2022; 253: 124219. https://doi.org/10.1016/j.energy.2022.124219.

[5] S. Negarestani, M. Fotuhi-Firuzabad, M. Rastegar, A. Rajabi-Ghahnavieh. Optimal Sizing of Storage System in a Fast Charging Station for Plug-in Hybrid Electric Vehicles. *IEEE Transactions on Transportation Electrification* 2016; 2(4): 443-53. https://doi.org/10.1109/TTE.2016.2559165.

[6] R. Sa'adati, M. Jafari-Nokandi, J. Saebi. Allocation of RESs and PEV Fast-Charging Station on Coupled Transportation and Distribution Networks. *Sustainable Cities & Society* 2021; 65: 102527. https://doi.org/10.1016/j.scs.2020.102527.

[7] A. Hussain, V.-H. Bui, H.-M. Kim. Optimal Sizing of Battery Energy Storage System in a Fast EV Charging Station Considering Power Outages. *IEEE Transactions on Transportation Electrification* 2020; 6(2): 453-63. https://doi.org/10.1109/TTE.2020.2980744.

[8] P. Mirhoseini, N. Ghaffarzadeh. Economic battery sizing and power dispatch in a grid-connected charging station using convex method. *Journal of Energy Storage* 2020; 31: 101651. https://doi.org/10.1016/j.est.2020.101651.

[9] C. Shao, T. Qian, Y. Wang, X. Wang. Coordinated Planning of Extreme Fast Charging Stations and Power Distribution Networks Considering On-Site Storage. *IEEE Transactions on Intelligent Transportation Systems* 2021; 22(1): 493-504. https://doi.org/10.1109/TITS.2020.3016765.

[10] M. Moradzadeh, M.M.A. Abdelaziz. A Stochastic Optimal Planning Model for Fully Green Stand-Alone PEV Charging Stations. *IEEE Transactions on Transportation Electrification* 2021; 7(4): 2356-75. https://doi.org/10.1109/TTE.2021.3069438.

[11] O. Hafez, K. Bhattacharya. Optimal design of electric vehicle charging stations considering various energy resources. *Renewable Energy* 2017; 107: 576-89. https://doi.org/10.1016/j.renene.2017.01.066.

[12] HOMER analysis. Online, available at: https://analysis.nrel.gov/homer/, (accessed on May 12, 2023).

[13] R. Xie, W. Wei, M.E. Khodayar, J. Wang, S. Mei. Planning Fully Renewable Powered Charging Stations on Highways: A Data-Driven Robust Optimization Approach. *IEEE Transactions on Transportation Electrification* 2018; 4(3): 817-30. https://doi.org/10.1109/TTE.2018.2849222.

[14] W. ur Rehman, R. Bo, H. Mehdipourpicha, J.W. Kimball. Sizing battery energy storage and PV system in an extreme fast charging station considering uncertainties and battery degradation. *Applied Energy* 2022; 313: 118745. https://doi.org/10.1016/j.apenergy.2022.118745.

[15] Y. Amry, E. Elbouchikhi, F.L. Gall, M. Ghogho, S.E. Hani. Optimal sizing and energy management strategy for EV workplace charging station considering PV and flywheel energy storage system. *Journal of Energy Storage* 2023; 62: 106937. https://doi.org/10.1016/j.est.2023.106937.

[16] Y. Zhou, P.D. Lund. Peer-to-peer energy sharing and trading of renewable energy in smart communities-trading pricing models, decision-making and agent-based collaboration. *Renewable Energy* 2023; 207: 177-93. https://doi.org/10.1016/j.renene.2023.02.125.

[17] Y. Zhou. A dynamic self-learning grid-responsive strategy for battery sharing economy-multi-objective optimisation and posteriori multi-criteria decision making. *Energy* 2023; 266: 126397. https://doi.org/10.1016/j.energy.2022.126397.

[18] D. Yan, C. Ma. Stochastic planning of electric vehicle charging station integrated with photovoltaic and battery systems. *IET Generation, Transmission & Distribution* 2020; 14(19): 4217-24. https://doi.org/10.1049/iet-gtd.2019.1737.

[19] J.A. Domínguez-Navarro, R. Dufo-López, J.M. Yusta-Loyo, J.S. Artal-Sevil, J.L. Bernal-Agustín. Design of an electric vehicle fast-charging station with integration of renewable energy and storage systems. *International Journal of Electrical Power & Energy Systems* 2019; 105: 46-58. https://doi.org/10.1016/j.ijepes.2018.08.001.

[20] N. G. Paterakis, O. Erdinç, A.G. Bakirtzis, J.P.S. Catalão. Optimal Household Appliances Scheduling Under Day-Ahead Pricing and Load-Shaping Demand Response Strategies. *IEEE Transactions on Industrial Informatics* 2015; 11(6): 1509-19. https://doi.org/10.1109/TII.2015.2438534.

[21] Y. Zhou. Energy sharing and trading on a novel spatiotemporal energy network in Guangdong-Hong Kong-Macao Greater Bay Area. *Applied Energy* 2022; 318: 119131. https://doi.org/10.1016/j.apenergy.2022.119131.

[22] J. Liu, Y. Zhou, H. Yang, H. Wu. Uncertainty energy planning of net-zero energy communities with peer-to-peer energy trading and green vehicle storage considering climate changes by 2050 with machine learning methods. *Applied Energy* 2022; 321: 119394. https://doi.org/10.1016/j.apenergy.2022.119394.

[23] S. Mandal, B.K. Das, N. Hoque. Optimum sizing of a stand-alone hybrid energy system for rural electrification in Bangladesh. *Journal of Cleaner Production* 2018; 200: 12-27. https://doi.org/10.1016/j.jclepro.2018.07.257.

[24] Y. Zhou. Sustainable energy sharing districts with electrochemical battery degradation in design, planning, operation and multi-objective optimization. *Renewable Energy* 2023; 202: 1324-41. https://doi.org/10.1016/j.renene.2022.12.026.

[25] E.S. Pinto, L.M. Serra, A. Lázaro. Evaluation of methods to select representative days for the optimization of polygeneration systems. *Renewable Energy* 2020; 151: 488-502. https://doi.org/10.1016/j.renene.2019.11.048.

[26] M. Tostado-Véliz, A.R. Jordehi, S.A. Mansouri, F. Jurado. A two-stage IGDT-stochastic model for optimal scheduling of energy communities with intelligent parking lots. *Energy* 2023; 263(D): 126018. https://doi.org/10.1016/j.energy.2022.126018.

[27] M. Tostado-Véliz, H.M. Hasanien, A.R. Jordehi, R.A. Turky, F. Jurado. Risk-averse optimal participation of a DR-intensive microgrid in competitive clusters considering response fatigue. *Applied Energy* 2023; 339: 120960. https://doi.org/10.1016/j.apenergy.2023.120960.

[28] Y. Zhou. Transition towards carbon-neutral districts based on storage techniques and spatiotemporal energy sharing with electrification and hydrogenation. *Renewable & Sustainable Energy Reviews* 2022; 162: 112444. https://doi.org/10.1016/j.rser.2022.112444.

[29] Y. Zhou. Incentivising multi-stakeholders' proactivity and market vitality for spatiotemporal microgrids in Guangzhou-Shenzhen-Hong Kong Bay Area. *Applied Energy* 2022; 328: 120196. https://doi.org/10.1016/j.apenergy.2022.120196.

[30] F. Fan, R. Zhang, Y. Xu, S. Ren. Robustly Coordinated Operation of an Emission-free Microgrid with Hybrid Hydrogen-battery Energy Storage. *CSEE Journal of Power and Energy Systems* 2022; 8(2): 369-79. https://doi.org/10.17775/CSEEJPES.2021.04200.

[31] Iberdrola. Charging Points for Electric Cars. Online, available at: https://www.iberdrola.es/en/smart-mobility/recharge-outside-the-house, (accessed on May. 15, 2023).

[32] S. Sarfarazi, S. Mohammadi, D. Khastieva, M.R. Hesamzadeh, V. Bertsch, D. Bunn. An optimal real-time pricing strategy for aggregating distributed generation and battery storage systems in energy communities: A stochastic bilevel optimization approach. *International Journal of Electrical Power & Energy Systems* 2023; 147: 108770. https://doi.org/10.1016/j.ijepes.2022.108770.

[33] Y. Zhou. Low-carbon transition in smart city with sustainable airport energy ecosystems and hydrogen-based renewable-grid-storage-flexibility. *Energy Reviews* 2022; 1: 100001. https://doi.org/10.1016/j.enrev.2022.100001.

[34] Y. Cao, W. Wei, S. Mei, M. Shafie-khah, J.P.S. Catalão. Analyzing and Quantifying the Intrinsic Distributional Robustness of CVaR Reformulation for Chance-Constrained Stochastic Programs. *IEEE Transactions on Power Systems* 2020; 35(6): 4908-11. https://doi.org/10.1109/TPWRS.2020.3021285.

[35] C. Ruiz, A.J. Conejo. Robust transmission expansion planning. *European Journal of Operational Research* 2015; 242(2): 390-401. https://doi.org/10.1016/j.ejor.2014.10.030.

[36] Gurobi Optimization L.L.C. Gurobi Optimizer Reference Manual, 2021. Online, available at: https://www.gurobi.com, (accessed on May. 15, 2023).

[37] European Comission. Photovoltaic Geographical Information System. Online, available at: https://re.jrc.ec.europa.eu/pvg_tools/en/tools.html, (accessed on May. 15, 2023).

[38] Engie. Historical data reports. Online, available at: https://www.engieresources.com/historical-data#reports_anchor, (accessed on May. 15, 2023).

[39] M. Tostado-Véliz, P. Arévalo, F. Jurado. An optimization framework for planning wayside and on-board hybrid storage systems for tramway applications. *Journal of Energy Storage* 2021; 43: 103207. https://doi.org/10.1016/j.est.2021.103207.

[40] Motorpasion. Cuánto cuesta cargar un coche eléctrico con las tarifas de la luz que hay en España en 2022 (in Spanish). Online, available at: https://www.motorpasion.com/coches-hibridos-alternativos/cuanto-cuesta-cargar-coche-electrico-tarifas-luz-espana-2021-20210607, (accessed on May. 15, 2023).